Combustion and Flame 162 (2015) 4649–4659

Contents lists available at ScienceDirect

Combustion and Flame

journal homepage: www.elsevier.com/locate/combustflame

Atom force microscopy analysis of the morphology, attractive force, adhesive force and Young's modulus of diesel in-cylinder soot particles

Nan Chen [a], Chonglin Song [a,*], Gang Lv [a], Jinou Song [a], Junhua Gao [b], Zhongrong Zhang [b]

[a] State Key Laboratory of Engines, Tianjin University, Tianjin 300072, China
[b] China Automotive Technology & Research Center, Tianjin 300300, China

ARTICLE INFO

Article history:
Received 21 May 2015
Revised 22 September 2015
Accepted 22 September 2015
Available online 21 October 2015

Keywords:
Diesel in-cylinder soot particles
Atomic force microscopy
Morphology
Attractive force
Adhesive force
Young's modulus

ABSTRACT

In this paper, the morphology, attractive force (F_{at}), adhesive force (F_{ad}) and Young's modulus (E_Y) of diesel in-cylinder soot particles sampled by a total cylinder sampling system were studied using atom force microscopy. In each combustion phase, the equivalent diameter (*ED*), F_{at}, F_{ad}, adhesion energy and E_Y present broad distributions. The pattern of *ED* distribution in the late combustion phase is similar to that in the late diffusion combustion phase, especially in the range of $ED < 10$ nm, suggesting that the particle size distribution changes little after the late diffusion combustion phase. Most isolated soot particles in each combustion phase possess a very low sphericity ratio. Three types of force curves are discovered for in-cylinder particles, and are introduced to identify the particle types. For the test carbonized soot particles, the *SR* appears to increase with an increase in *ED* in each combustion phase, and the *AED* shows a similar trend to that for all test particles during the combustion process. Due to the presence of plastic deformation for the nascent soot particles and the penetration for the liquid materials during the force measurement, the carbonized primary soot particles are employed for force analysis. As the combustion proceeds, the population-averaged values of F_{at} and F_{ad} show opposite trends; the attractive force, which is mainly driven by the Van der Waals force, gradually decreases. During the combustion process, the population-averaged adhesion energy decreases to a minimum in the late premixed combustion phase after which it then increases. The initial increase in the population-averaged Young's modulus (AE_Y) is followed by a decrease before gradually increasing again from the early diffusion combustion phase. The AE_Y shows a negative correlation with the fringe separation distance in the soot structure.

1. Introduction

Soot particles are an important combustion-generated pollutant. Their adverse effects on the environment and human health [1,2] and an incomplete understanding of their formation and evolution ensure that they continue to receive much attention in the field of combustion research. Soot formation and evolution involves six commonly identified processes—pyrolysis, nucleation, coalescence, surface growth, agglomeration, and oxidation—which all occur within a few milliseconds [3]. Associated with these processes are the accompanying changes in the physicochemical properties of the soot particles, including morphology [4–7], charge distribution [8–10], nanostructure [11–15], and surface functional groups [16,17]. Therefore, knowledge of these properties is essential for the understanding of the soot formation mechanism.

To date, the physicochemical properties of soot particles have been studied extensively, and the effects of temperature, fuel identity, residence time and pressure on these properties have been explored through experiments [4–17] and simulations [18–21]. These studies evidenced that the physicochemical properties were highly correlated with the temperature, fuel identity, residence time and pressure of flame, and significantly influenced the formation and evolution of soot particles. For instance, the nanostructural differences in the planar structure and orderliness of the graphene within the soot particles were found to be dependent on the fuel identity and the synthesis or combustion conditions [12,13]. Simultaneously, changes in the planar structure and orderliness of the graphene also in turn affect the oxidative reactivity of the soot [11,14].

The attractive (F_{at}) and adhesive (F_{ad}) forces between soot particles are important physicochemical features of soot particles that help to explain their coagulation and aggregation [22,23] and can be obtained from atomic force microscopy (AFM). Indeed, AFM cannot only furnish 3D images of soot particles [4,5,7], but also measure the force curves. The force curves from AFM have been used as a fundamental tool in several fields of research (such as materials

* Corresponding author. Fax: +86 22 27403750.
E-mail address: songchonglin@tju.edu.cn (C. Song).

http://dx.doi.org/10.1016/j.combustflame.2015.09.025
0010-2180/

Nomenclature

A	Hamaker constant (J)
AED	population-averaged equivalent diameter (nm)
AE_Y	population-averaged Young modulus (MPa)
AF_{ad}	population-averaged adhesive force (nN)
AF_{at}	population-averaged attractive force (nN)
AW_{ad}	population-averaged adhesion energy (J)
$AHRR$	apparent heat release rate (J/deg)
CA	crank angle (°)
D	base diameter of soot particle (nm)
d	cantilever deflection (nm)
d_p	mean primary particle diameter (nm)
d_s	shortest distance between the tip and soot particle (nm)
E	interactive energy (J)
ED	equivalent diameter (nm)
E_T	thermal kinetic energy (J)
E_Y	Young's modulus (MPa)
F	interactive force (nN)
F_{ad}	adhesive force (nN)
K	Boltzmann constant (J/K)
F_{at}	attractive force (nN)
F_{vdw}	Van der Waals force (nN)
k_c	cantilever spring constant (N/m)
P	cylinder pressure (Mpa)
R	radius (nm)
R^2	square of the linear correlation coefficient
RH	relative humidity
S	photodetector sensitivity (V/nm)
SR	sphericity ratio
T	temperature (K)
V	photodiode voltage (V)
W_{ad}	adhesion energy (J)

Acronyms

ATDC	after top dead center
AFM	atomic force microscopy
HAB	height above the burner
SEM	scanning electron microscope
SPIP	scanning probe image processor
TCSS	total cylinder sampling system
TEM	transmission electron microscope

engineering, surface science, biology and biochemistry) [24], but rarely in soot particle analysis. In the present work, AFM was employed to measure F_{at}, F_{ad} and the adhesion energy (W_{ad}) between diesel in-cylinder soot particle and the AFM tip. The evolving 3D soot morphology and the Young's modulus (E_Y) for the particles were also characterized and are discussed to provide a more holistic view of the formation nature of soot particles during diesel combustion.

2. Experimental

2.1. Sampling system

Experiments were performed on a 5.79 L heavy-duty diesel engine with six cylinders. This engine was equipped with a high-pressure, common-rail fuel injection system and a turbocharged/inter-cooled air intake system, and powered up to 132 kW at a maximum speed of 2600 rpm. The sixth cylinder was modified to develop a total cylinder sampling system (TCSS) that was used to sample soot particles from the combustion chamber. Here, an aluminum alloy diaphragm was used to seal the engine cylinder head as a sampling valve. At a pre-set crank angle (CA) during a sampling cycle, the aluminum alloy diaphragm was instantaneously cut by an electromagnet-actuated tube cutter and the cylinder contents were rapidly discharged from the cylinder into a sampling bag. The sampled gas mixture was immediately quenched and diluted by mixing with high-pressure nitrogen to obtain a temperature below 52 °C. According to our prior study [15], the dilution ratio used in the present work was set at 120:1 to abate the aggregation and oxidation of soot particles during the sampling process. A detailed description of this apparatus and sampling procedure has previously been reported [13,15,16]. An ultra-low sulfur diesel fuel was used, and the properties of this fuel were listed in Table 1. Engine was operated at 1000 rpm with the air-intake temperature of 318 K and the fuel–air ratio of 0.467. The start and end of fuel injection were set at −7°CA and 0.5°CA after top dead center (ATDC) respectively, and the fuel injection pressure was 100 MPa. The pressure (P), temperature (T) and apparent heat release rate ($AHRR$) throughout the combustion process are shown in Fig. 1. To characterize the in-cylinder soot particles, five sampling points were chosen to represent the different diesel combustion phases according to the plots of P and $AHRR$. The determination of the diesel combustion phases followed the method suggested by Heywood [25]. The five sampling points corresponded to the onset of the premixed combustion phase (−0.5°CA ATDC), the end of the premixed combustion phase (2.5°CA ATDC), the early diffusion combustion phase (7°CA ATDC), the late diffusion combustion phase (18°CA ATDC) and the late combustion phase (24.5°CA ATDC). Samples from the sampling bag were collected onto a mica substrate (diameter 9 mm, roughness ≤0.2 nm) for analysis.

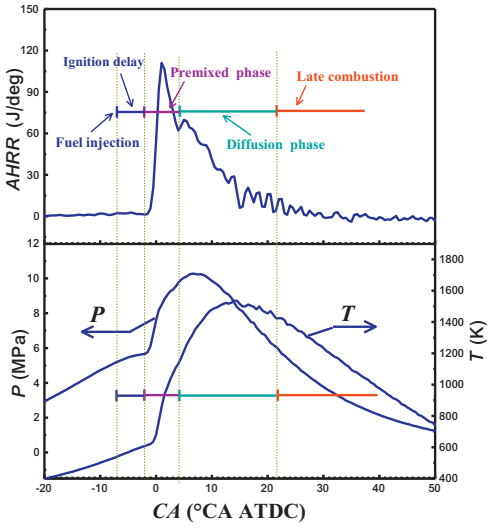

Fig. 1. In-cylinder gas pressure (P), temperature (T), and apparent heat release rate ($AHRR$) diagram identifying different diesel combustion phases.

Table 1
Properties of test fuel.

Cetane umber	Density (kg/m^3)	Sulfur content (mg/kg)	Polycyclic aromatic hydrocarbon content (%)	Solidifying point (°C)	Flashing point (°C)
51.2	831	7.8	1.9	< 0	70.5